sustainability

MDPI

Article

Creating Sustainable Flood Maps Using Machine Learning and Free Remote Sensing Data in Unmapped Areas

Héctor Leopoldo Venegas-Quiñones [1,*], Pablo García-Chevesich [2,3], Rodrigo Valdés-Pineda [1], Ty P. A. Ferré [1], Hoshin Gupta [1], Derek Groenendyk [1], Juan B. Valdés [1], John E. McCray [2] and Laura Bakkensen [4]

1 Hydrology and Water Resources Department, University of Arizona, 1133 E James E. Rogers Way, Tucson, AZ 85721, USA; rvaldes@arizona.edu (R.V.-P.); tyferre@arizona.edu (T.P.A.F.); hoshin@arizona.edu (H.G.); derek.groenendyk@gmail.com (D.G.); jbv1969@gmail.com (J.B.V.)
2 Department of Civil and Environmental Engineering, Colorado School of Mines, 1500 Illinois St., Golden, CO 80401, USA; pablogarcia@mines.edu (P.G.-C.); jmccray@mines.edu (J.E.M.)
3 Intergubernmental Hydrological Programme, United Nations Educational, Scientific, and Cultural Organization, Montevideo 11200, Uruguay
4 School of Government and Public Policy, University of Arizona, 1145 S Campus Drive, Tucson, AZ 85721, USA; laurabakkensen@arizona.edu
* Correspondence: venegasquinones@arizona.edu

Abstract: This study leverages a Random Forest model to predict flood hazard in Arizona, New Mexico, Colorado, and Utah, focusing on enhancing sustainability in flood management. Utilizing the National Flood Hazard Layer (NFHL), an intricate flood map of Arizona was generated, with the Random Forest Classification algorithm assessing flood hazard for each grid cell. Weather variable predictions from TerraClimate were integrated with NFHL classifications and Digital Elevation Model (DEM) analyses, providing a comprehensive understanding of flood dynamics. The research highlights the model's capability to predict flood hazard in areas lacking NFHL classifications, thereby supporting sustainable flood management by elucidating weather's influence on flood hazard. This approach aligns with sustainable development goals by aiding in resilient infrastructure design and informed urban planning, reducing the impact of floods on communities. Despite recognizing constraints such as input data precision and the model's potential limitations in capturing complex variable interactions, the methodology offers a robust framework for flood hazard evaluation in other regions. Integrating diverse data sources, this study presents a valuable tool for decision-makers, supporting sustainable practices, and enhancing the resilience of vulnerable regions against flood hazards. This integrated approach underscores the potential of advanced modeling techniques in promoting sustainability in environmental hazard management.

Keywords: machine learning; flood hazard assessment; remote sensing; random forest model; flood mapping

Citation: Venegas-Quiñones, H.L.; García-Chevesich, P.; Valdés-Pineda, R.; Ferré, T.P.A.; Gupta, H.; Groenendyk, D.; Valdés, J.B.; McCray, J.E.; Bakkensen, L. Creating Sustainable Flood Maps Using Machine Learning and Free Remote Sensing Data in Unmapped Areas. *Sustainability* **2024**, *16*, 8918. https://doi.org/10.3390/su16208918

Academic Editor: Xander Wang

Received: 14 August 2024
Revised: 10 October 2024
Accepted: 11 October 2024
Published: 15 October 2024

1. Introduction

Flood occurrences and intensity are rising, significantly impacting various regions [1]. Changes in rainfall and land use amplify flood hazards [2], with long-lasting effects such as soil erosion, water pollution, and disease spread [3,4]. Understanding flood trends and causes is crucial for developing effective hazard reduction and adaptation strategies [5]. Floods can have severe economic and human impacts [6]. A Stanford study found that increased rainfall caused a third of the USD 199 billion flood damages in the U.S. from 1988 to 2017 [7]. Floods also result in fatalities, physical harm, and psychological distress [7], with 1336 flood-related deaths reported in the U.S. from 2000 to 2010 [8]. Demographic factors like age and income influence flood mortality rates [9]. Accurate, current flood maps are essential for effective flood hazard management and decision-making at all levels [10,11].

These maps inform land use planning, infrastructure development, and emergency response. They also raise public awareness and promote proactive measures [11,12].

The rising frequency and severity of floods globally, driven by climate change, urbanization, and deforestation, underscore the need for reliable flood maps [13]. Advances in technology and data collection have led to more detailed and accurate flood maps, using tools like remote sensing and GIS mapping [14]. These maps are crucial for saving lives, protecting property, and guiding decision-making. In the U.S., the Federal Emergency Management Agency (FEMA) produces flood maps to manage flood hazards [11,15], including Flood Insurance Rate Maps (FIRMs), which use diverse data sources to identify flood hazard areas (Figure 1) [16,17]. A flood hazard map illustrates areas potentially affected by flood events, highlighting regions prone to flooding based on historical data, topography, and hydrological models. Conversely, a flood risk map integrates hazard information with socio-economic factors, assessing the potential impact on populations, infrastructure, and assets. It considers not only the likelihood of flooding but also the vulnerability and exposure of the affected area, providing a more comprehensive view of the potential consequences. FEMA classifies flood hazard areas into various zones to help communities and individuals understand their risk and make informed decisions [16]. The cost of creating and maintaining flood maps is significant, influenced by factors like area size, detail required, and data availability [18]. Developing these maps involves substantial data collection, modeling, and expert analysis [16,19]. FEMA's national FIRM creation could cost up to USD 11.8 billion, with annual maintenance costs between USD 107 million and USD 480 million [20].

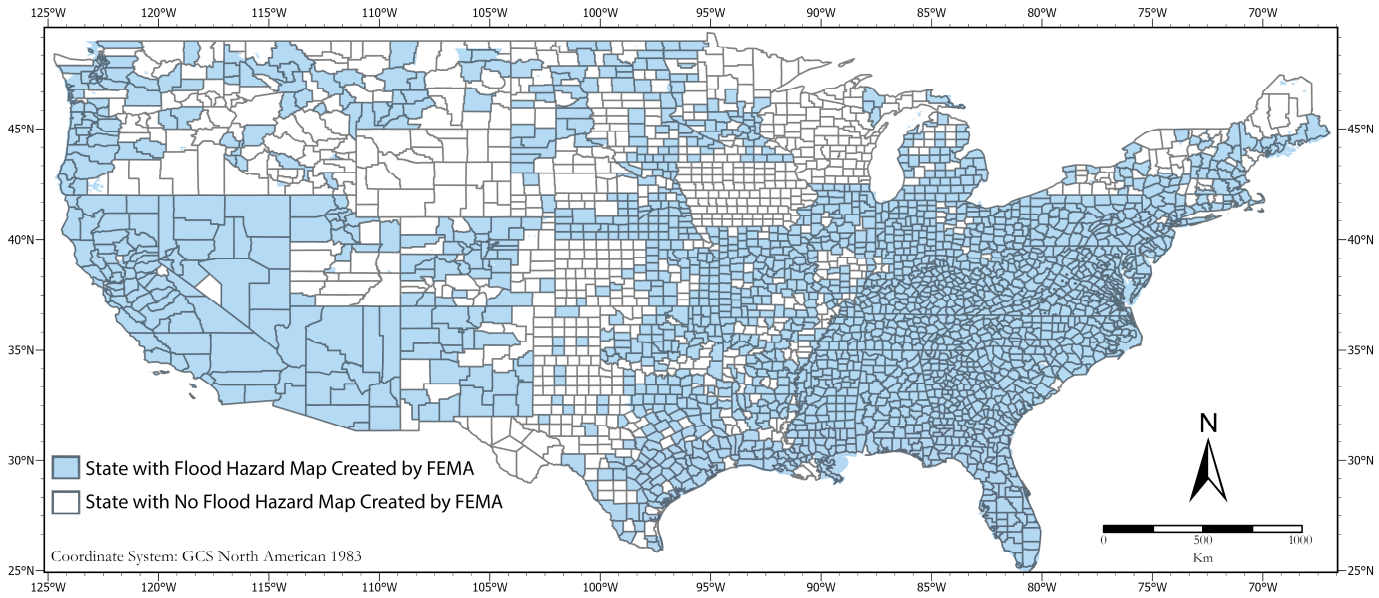

Figure 1. Geographic Distribution of FEMA Flood Insurance Rate Maps in the United States.

Approximately 80% of those at risk from river floods live in 15 developing countries, including India, Bangladesh, China, and Vietnam, which often lack resources to mitigate flood impacts [21]. In these countries, the absence of flood hazard maps exacerbates disaster readiness and response challenges.

Machine Learning, Random Forest Classification, Research, and Results

Advanced technologies like GIS, cloud computing, and machine learning (ML) are revolutionizing flood hazard map creation, making it quicker, more cost-effective, and highly accurate [22]. ML uncovers hidden patterns in data, enhancing flood forecasting, estimating maximum flood depth, and providing alerts [23,24]. The Google Flood Hub exemplifies ML's potential, offering near-instantaneous flood forecasts worldwide by

combining ML algorithms with satellite data [25]. However, integrating FEMA flood maps with ML for global applicability remains a challenge.

Random Forest (RF) models, a type of ML, predict flood events by combining results from multiple regression trees based on sampled data [26]. RF has been used in remote sensing to classify land cover and predict natural events like forest fires [27], urban areas [28], agricultural land [29], landslides [30], and floods [31,32]. Recent research focuses on using RF with remote sensing and national data to model floodplains and predict flood damage accurately.

Despite progress, the global application of these models is limited by data availability. For example, Collins and Sanchez's work using U.S. national data restricts applicability outside the U.S. [33]. Woznicki and Baynes developed RF models for U.S. watersheds, showing promise for floodplain mapping but limited by the same data constraints [17].

The goal of using RF in flood hazard mapping is to create cost-effective, fast models applicable worldwide. By analyzing diverse data sets, RF aims to produce accurate flood maps for data-scarce regions, improving flood hazard management and safety. This research, focusing on Arizona, provides accurate flood maps to help local communities prepare for floods. All data is publicly accessible through an ArcGIS Pro 3.3.2 interactive map, encouraging further research and aiding those in flood-prone areas. Thus, this paper focuses solely on the creation of flood hazard maps, emphasizing the identification, and characterization of areas at risk of flooding. By doing so, it provides a critical foundation for understanding flood dynamics and informing subsequent risk assessments and mitigation efforts.

2. Methodology

The methodological process is depicted in Figure 2. Initially, topographic and weather data from Arizona are used to calibrate the model and create a grid of cells with designated National Flood Hazard Layer (NFHL) values. The RF Classification algorithm estimates the NFHL for each cell, and this calibrated model is then applied to generate NFHL values for countries in New Mexico, Colorado, and Utah. The final product is an interactive ArcGIS map available for public use.

2.1. Current Data in Arizona, Utah, Colorado, and New Mexico

This study employs the NFHL as the principal data source for flood map analysis in Arizona. The NFHL, a geospatial database developed by FEMA, offers current information on flood hazards across the United States, including Arizona. FEMA's flood zone classifications are essential in understanding flood risks across different regions. Zone A represents areas with a 1% annual chance of flooding, also known as the 100-year floodplain, where no detailed flood elevations are provided. Zone AE also falls within the 100-year floodplain but includes specific base flood elevations, offering more precise risk assessments. Zone AH indicates areas with shallow flooding, typically ponding, with flood depths ranging from 1 to 3 feet. Zone AO is designated for areas with shallow flooding, usually sheet flow, with average depths of 1 to 3 feet. Zone D covers areas with possible but undetermined flood hazards, where no analysis has been conducted. Finally, Zone X represents areas of minimal flood risk, outside the 100-year and 500-year floodplains, where the likelihood of flooding is low. To initiate the analysis, the latest version of the Arizona NFHL was first procured. This database encompasses information on flood zones, base flood elevations, and floodway boundaries, among other flood hazard-related data. This data was extracted and processed to construct a high-resolution flood map of Arizona. In Arizona, these classifications encompass A, AE, AH, AO, D, X, and an "area not included" designation. It is crucial to note that all the counties in Arizona have been assessed and classified using the NFHL. Conversely, certain counties in the State of New Mexico have not yet undergone flood hazard analysis. Specifically, the counties of Catron, Hidalgo, Sierra, Torrance, Guadalupe, De Baca, Quay, Mora, Harding, and Union currently lack an NFHL classification (see Figure 3). Similar to the State of Colorado, Utah also has counties

that have not been classified by the National Flood Hazard Layer (NFHL). Specifically, the counties of Rich, Juab, Millard, Beaver, Iron, Kane, Garfield, Piute, Sevier, Emery, Wayne, San Juan, Grand, Duchesne, and Daggett currently lack an NFHL classification (Figure 3).

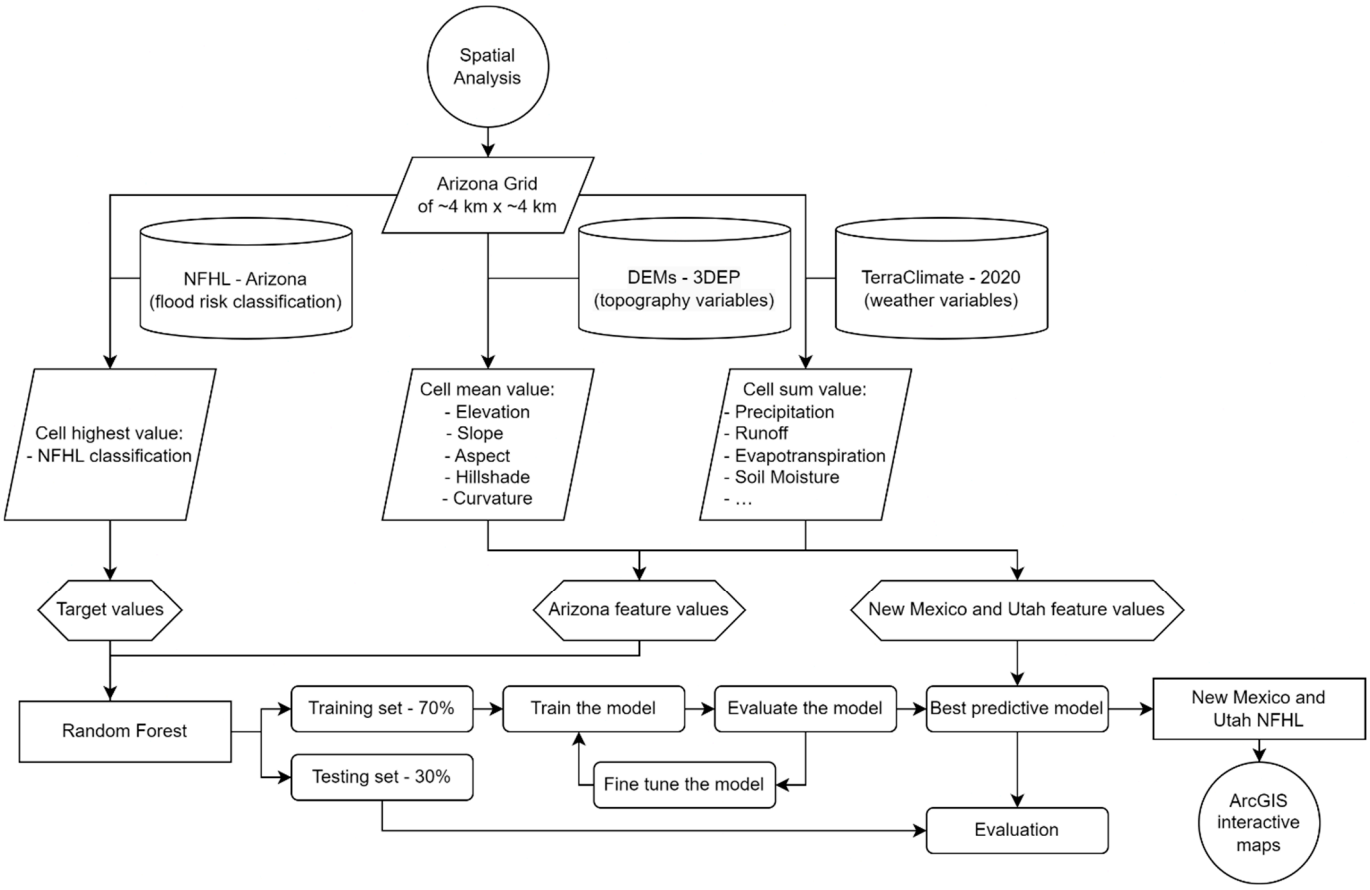

Figure 2. Flowchart showing the development of an RF-based model for estimating NFHL values in New Mexico, Colorado, and Utah using topographic and weather data.

2.2. Topographic Information

To precisely forecast flood hazard in regions without NFHL classifications, the highly detailed USGS 3D Elevation Program (3DEP) Standard DEMs were used. These DEMs supply crucial elevation data that were used to inform the RF model by estimating terrain parameters such as elevation, slope, aspect, hill shade, curvature, flow direction, and flow accumulation. Figure 4 illustrates the DEM analysis for Arizona.

2.3. Weather Information—TerraClimate (Remote Sensing Data)

To enhance our flood hazard analysis, estimations of weather variables from the TerraClimate dataset were integrated. These variables, including precipitation and temperature, can exert a significant influence on flood hazard in a specific area. TerraClimate offers gridded estimates of monthly climate and water balance variables at an approximate resolution of four kilometers. This data is compiled using a blend of weather station data, remote sensing, and other climate datasets, resulting in a comprehensive and precise depiction of climate patterns in a specific area. By integrating this data into our flood hazard analysis, a deeper understanding of the relationship between weather patterns and flood hazard in each area can be gained. It is crucial to highlight that only the 2020 weather information from TerraClimate was used, coinciding with the most recent update of the NFHL map of Arizona. This ensures that the obtained flood hazard analysis is grounded in the most recent and relevant data available. To encapsulate the total impact of weather on flood haz-

ard in each cell, the annual sum of each weather variable obtained from TerraClimate was calculated. This provided a holistic view of the overall influence of weather on flood hazard in each area. Figure 5 shows some of the weather variables obtained from TerraClimate for Arizona.

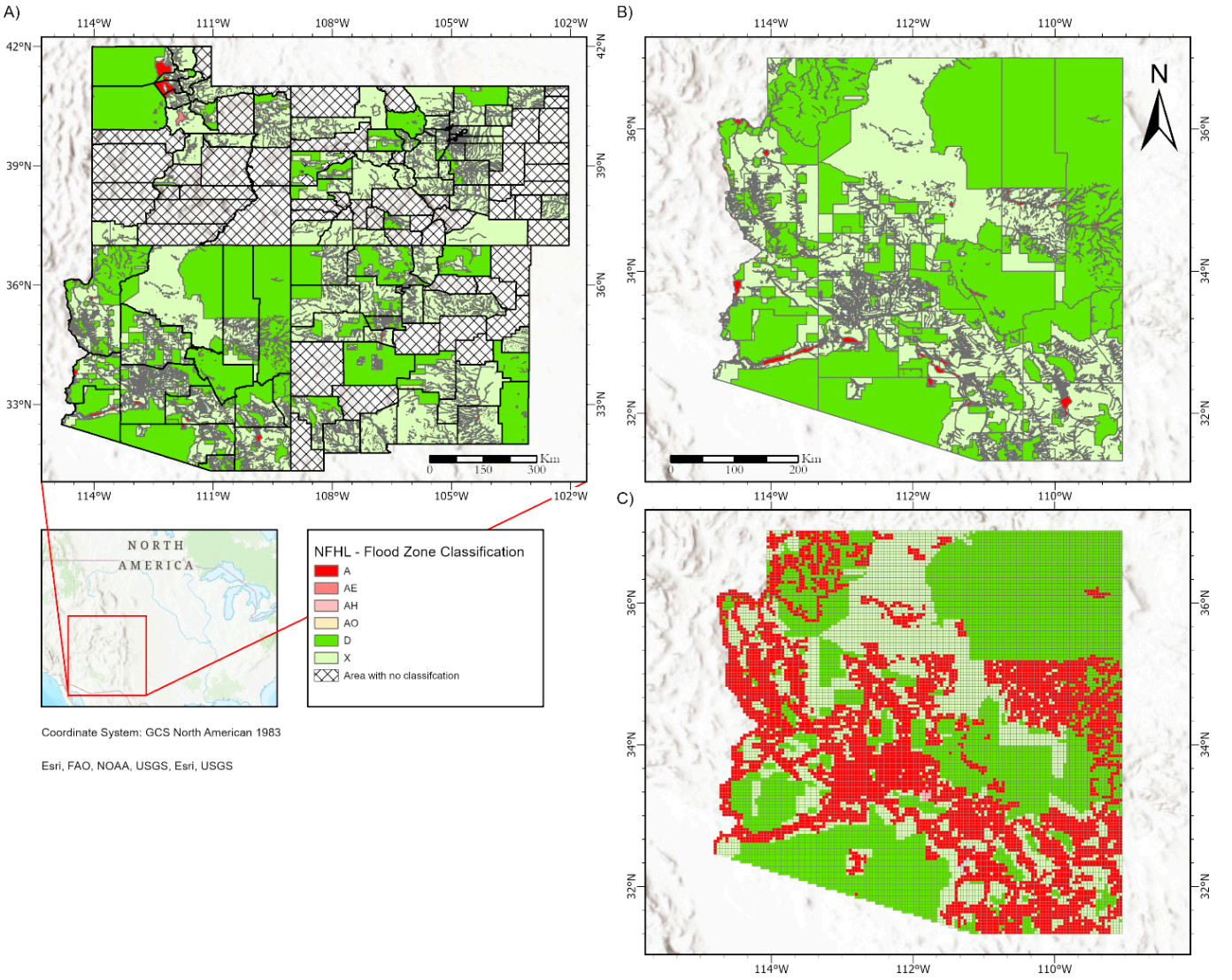

Figure 3. (**A**) National Flood Hazard Layer (NFHL) Analysis in Arizona, New Mexico, Colorado, and Utah: Extracting and Processing Data to Create High-Resolution Flood Maps. (**B**) NFHL Classification for Arizona. (**C**) NFHL-Based Flood Hazard Analysis in Arizona Using Grid Cell Classification for Arizona (worst-case threshold).

Thus, the topographic variables incorporated in this study encompass elevation, slope, aspect, hill shade, curvature, flow direction, and flow accumulation, as previously mentioned. It also included a range of meteorological variables sourced from TerraClimate such as total annual 2020 precipitation, runoff, soil moisture, snow water equivalent, actual evapotranspiration, climate water deficit, downward surface shortwave radiation, maximum and minimum temperatures, vapor pressure, wind speed, vapor pressure deficit, and the Palmer Drought Severity Index.

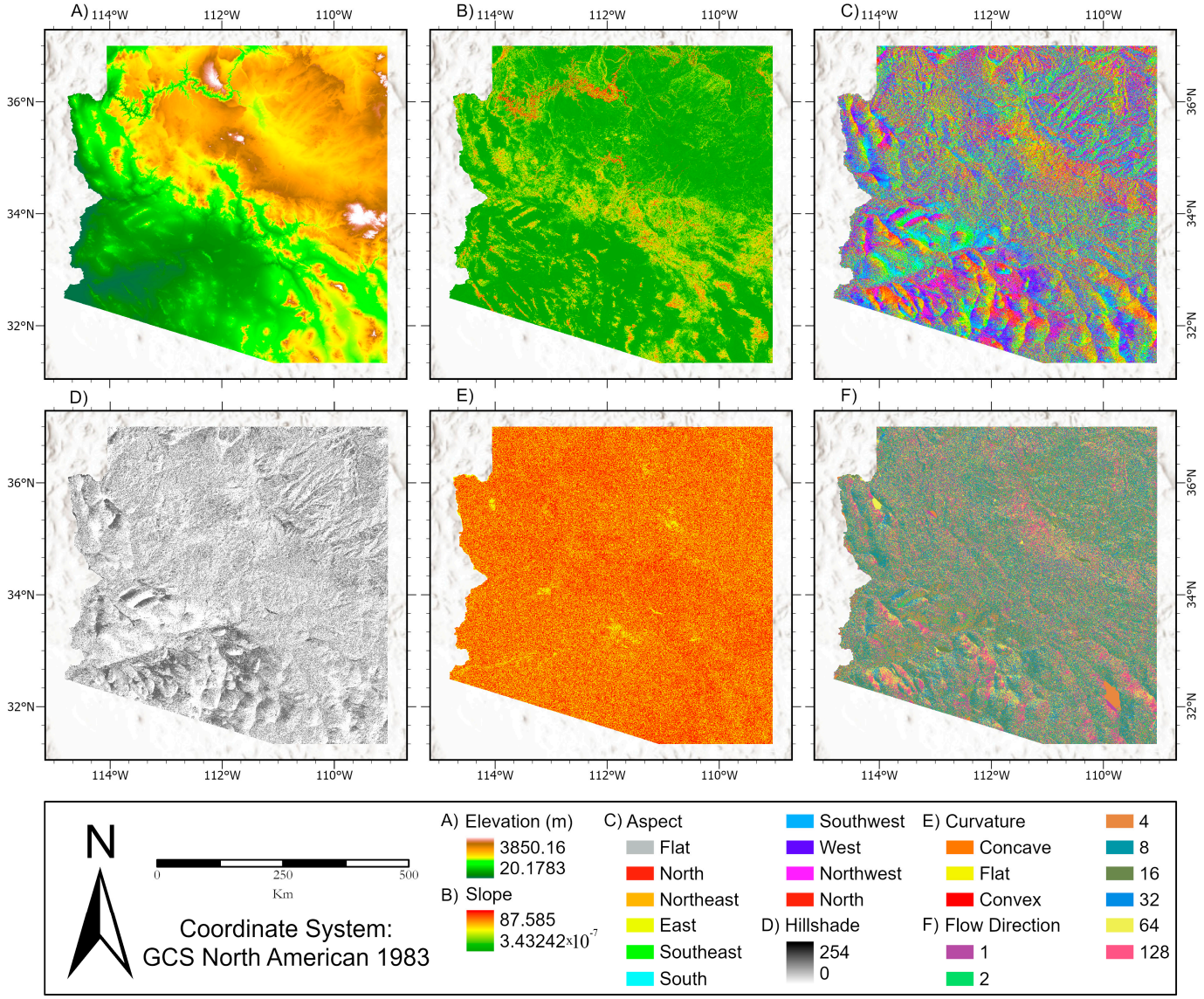

Figure 4. Digital Elevation Model (DEM) analysis of Arizona for flood hazard prediction using USGS 3D Elevation Program (3DEP).

2.4. Grid Creation

To incorporate the weather variable estimation from TerraClimate into the flood hazard analysis, a grid for Arizona that aligns with the resolution of TerraClimate was built. This facilitated the spatial alignment of the climate data with other information sources such as the NFHL classifications and DEM analysis. The grid that was developed consists of cells with a uniform spatial resolution, enabling the computation of climate variables for each cell. By employing a consistent grid, it standardized the data across the entire region, simplifying the analysis and comparison of different areas. As an integral part of the flood hazard analysis in Arizona, the NFHL classifications was used to ascertain the flood hazard for each cell in the grid. The highest NFHL classification within each cell is designated as the representation of the flood hazard. To evaluate flood hazard for each cell, four different thresholds were applied including the worst-case scenario, 5%, 10%, 25%, 50%, and 75%, based on the area of the classification in each cell. Under the worst-case scenario threshold, if any portion of a cell has a flood hazard level of A, the entire cell is deemed to have a flood hazard level of A (Figure 3C). For the 25% threshold, if the area of the cell with a flood

hazard level of A encompasses more than 25% of the cell, the entire cell is deemed to have a flood hazard level of A. This process was repeated with 5%, 10%, 50%, and 75% thresholds.

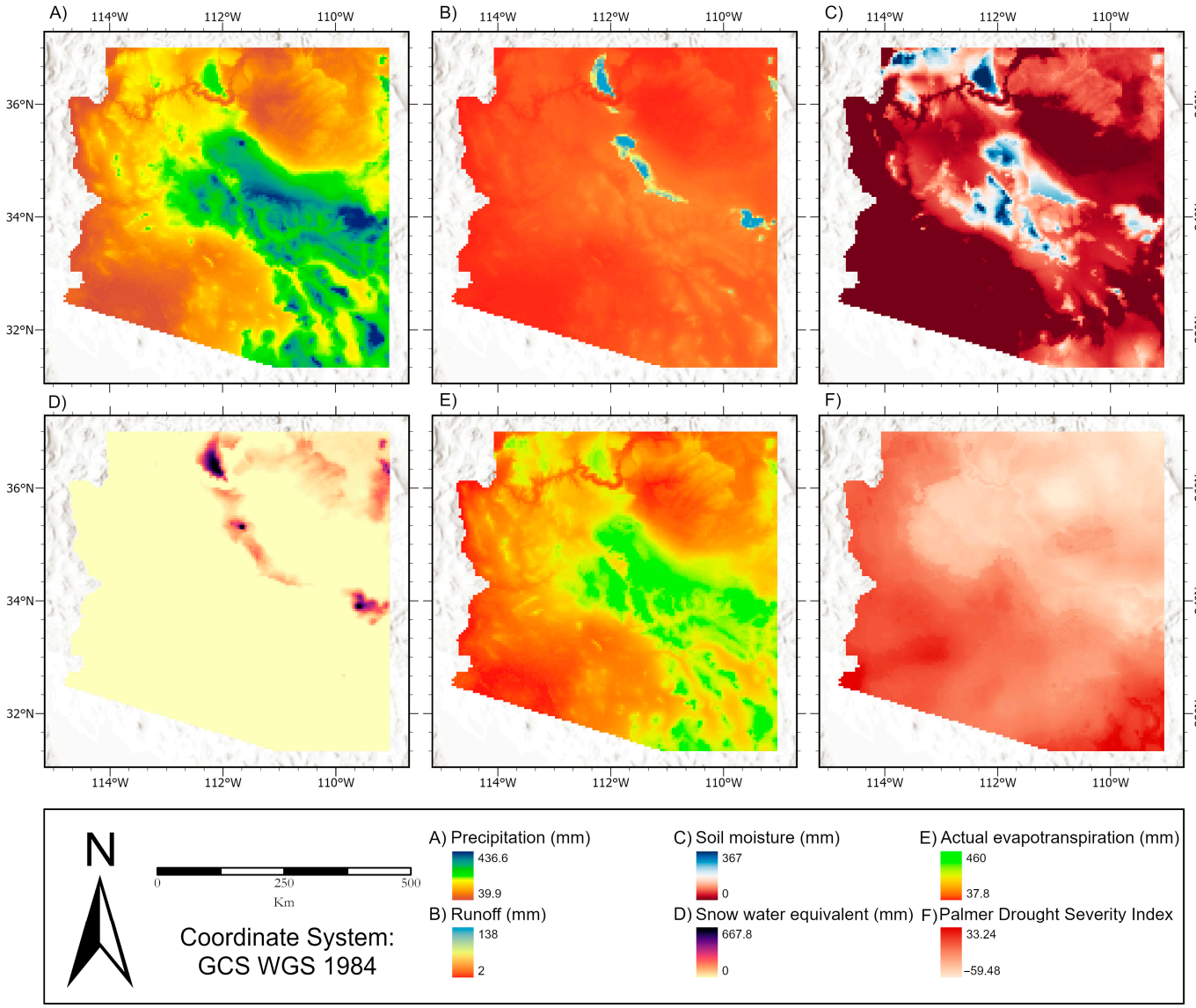

Figure 5. TerraClimate weather variables for Arizona.

The flood hazard assessment involved an evaluation of results obtained using various thresholds, aiming to identify the most suitable threshold for each grid in the study area. The chosen threshold plays a crucial role in enhancing the accuracy of flood hazard analysis and supporting decision-making in disaster risk management. The application of different thresholds enables the identification of optimal flood hazard levels within each cell, thereby improving the precision of flood hazard predictions. Subsequently, we combined the A and AE categories, resulting in the creation of a new merged category labelled "A". This consolidation serves the purpose of streamlining the flood hazard analysis process and facilitating a clearer understanding of the flood hazard associated with the areas under examination. Going forward, the "A" classification was used to represent areas with a 1% annual chance of flooding, regardless of the presence of base flood elevations. It was anticipated that this approach will contribute to a more efficient and comprehensive analysis of flood hazard in the affected regions. For instance, consider a cell in the grid situated in Phoenix, Arizona. This cell possesses a resolution of approximately 4 km × 4 km and encompasses multiple NFHL classifications including zones A and D. Using the

methodology of designating the highest NFHL classification within each cell, it would be attributed a flood hazard level of A to this cell, as it signifies the most severe flood hazard classification within that cell. This guarantees that the most critical flood hazard within the cell was captured and used to formulate the flood hazard predictions by applying various thresholds.

2.5. Random Forest Configuration

In this research, a RF Classification methodology was employed to estimate the NFHL for each cell in Arizona. Topographic and weather data for each cell were incorporated as input to the model. The dataset was partitioned into a training set comprising 70% of the data and a testing set comprising the remaining 30%. Scikit-Learn's RandomizedSearchCV was used, which conducted a random search of parameters within a specified range for each hyperparameter. Specifically, the parameter distribution of the number estimator (ranging from 10 to 500) was used, and the maximum number of trees (ranging from 2 to 20) to randomly sample 10 combinations of hyperparameters. A cross-validation approach with 10 folds was employed to assess the performance of each set of hyperparameters. Additionally, the Gini index was used to evaluate the importance of features and identify which input variables were most influential in predicting flood hazard. The Gini index is a metric used in decision trees to evaluate the quality of a split. It measures the degree of disorder or impurity in a dataset, where 0 represents perfect purity (all elements belong to a single class), and higher values indicate more impurity. Mathematically, the Gini index is expressed as:

$$Gini = 1 - \sum_{i=1}^{n} \left(p_i^2 \right)$$

Here, p_i^2 denotes the proportion of items classified as class i within the node, while n signifies the total number of classes. By discerning the pivotal features driving the model's predictive performance, we aim to enhance the accuracy and efficacy of flood hazard assessments, thereby contributing to more informed decision-making processes in flood management and mitigation strategies.

2.6. Predicting NFHL for New Mexico, Colorado, and Utah

Upon calibrating the RF model with the data from Arizona, it was employed to estimate the NFHL for each cell in the counties of New Mexico, Colorado, and Utah that were devoid of flood hazard information. Initially, the topography and weather for each cell were estimated, then fed these as inputs into the trained RF model to generate the NFHL.

Finally, using a calibrated RF model, the NFHL for each cell was estimated based on topographic and weather data. This data was then integrated into an interactive ArcGIS map, enhancing public understanding. This tool provides a straightforward means for visualizing and analyzing flood hazard across Arizona, New Mexico, Colorado, and Utah. The map, which is publicly accessible, serves as a valuable resource for local authorities, emergency management agencies, and residents in these regions for planning and preparedness purposes.

3. Results

3.1. Grid

In this study, Arizona was divided into 16,999 standardized cells, each with an area of 17.24 km^2. A flood hazard assessment was then conducted under a worst-case scenario to identify the most flood-prone areas. Under this scenario, 5906 cells were classified as A zones, with no cells in AH zones, and only six cells in AO zones. Additionally, 3263 cells were classified as D zones, while the remaining 7824 cells fell under X zones. These findings, along with other threshold scenarios, are detailed in Table 1. Notably, majority of the cells classified as A zones were identified under the worst-case scenario, underscoring the potential flood vulnerability of these areas under the strictest assessment. In contrast,

only 98 cells were classified as A zones under the 75% threshold evaluation, suggesting a comparatively lower flood hazard in these areas.

Table 1. Thresholds and Flood Hazard Classification Results for Arizona.

Threshold	A (A + AE)	AH	AO	X	D
Worst-case scenario	5906	0	6	3263	7824
5%	2888	3	23	5192	8893
10%	1677	3	25	6109	9185
25%	597	4	29	6994	9375
50%	205	4	31	7321	9438
75%	98	4	31	7321	9545
Sum of cells	11,371	18	145	36,200	54,260

Figure 6 illustrates an all-encompassing visual depiction of the flood hazard assessment outcomes for Arizona, considering various threshold parameters. The figure underscores the dynamic classification of diverse regions within the State, contingent on the analytical criteria employed. This offers detailed insight into the geographical distribution of flood hazard across the region.

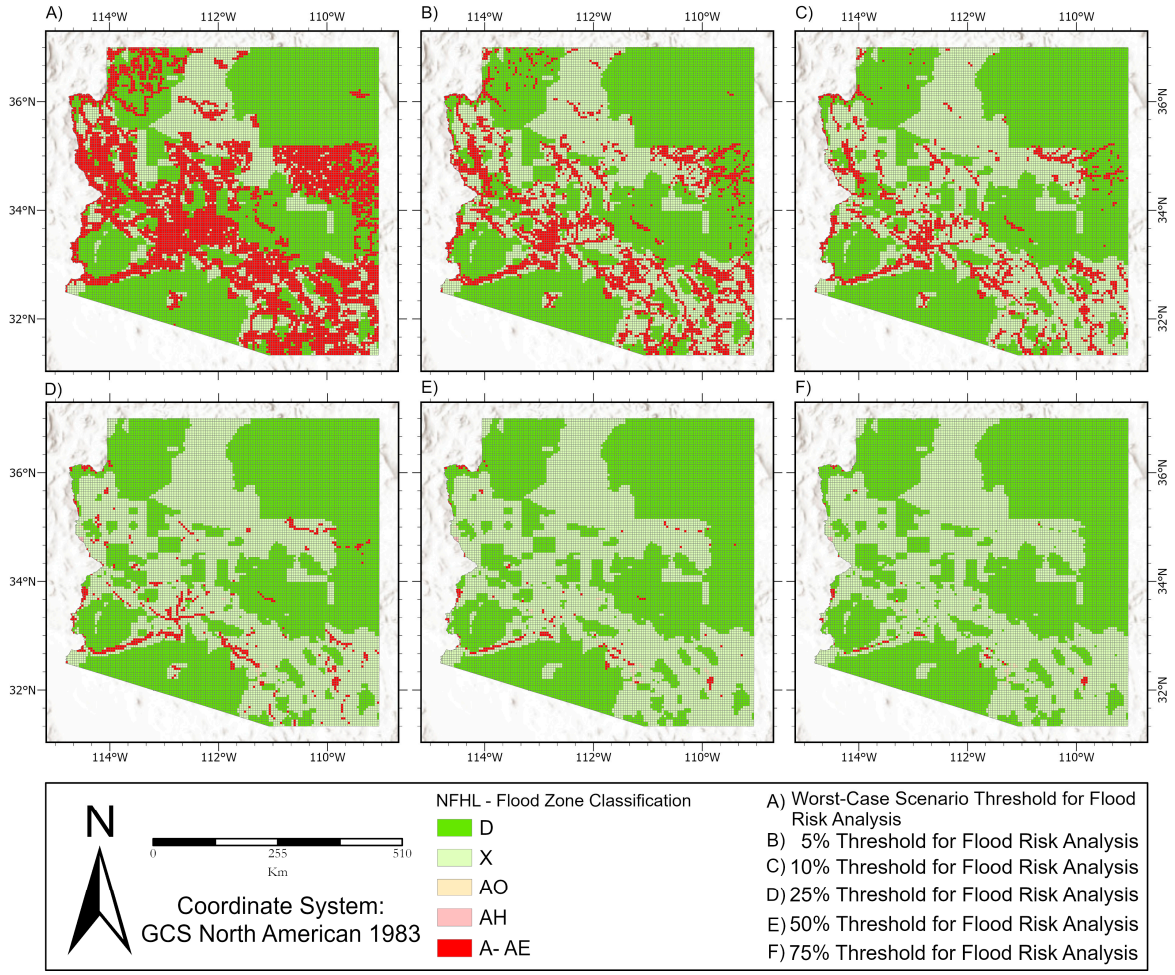

Figure 6. Flood hazard analysis results for Arizona: spatial distribution across different threshold settings.

3.2. Grid and TerraClimate Information Merge

To construct a predictive model for flood hazard, topographic and meteorological data for each flood hazard classification cell throughout Arizona was gathered. These data points served as features in the ML RF model, while the flood hazard classification of each cell was used as the target variable. This methodology enabled the creation of a flood hazard predictive model that was customized to the distinct attributes of Arizona's various regions. The integration of topographic and meteorological data into our model allowed us to consider a broad spectrum of factors influencing flood hazard, thereby enhancing the accuracy of the flood hazard predictions across the State. All these variables were employed as features in our RF Classifier model, with the flood hazard classification acting as the target variable. The total feature count for each flood hazard classification cell target was 19, inclusive of the aforementioned topographic and meteorological variables.

3.3. Random Forest

An RF Classifier was used to forecast the flood hazard categorization for each cell in Arizona. The model was calibrated using the RandomizedSearchCV method, which entails the selection of the optimal hyperparameters through repeated cycles of random parameter sampling. The outcomes are detailed in Table 2. The RF Classifier exhibited superior performance, with a Training Accuracy of 1.0 and a testing sample accuracy surpassing 0.8 for each threshold setting. To elucidate the performance metrics, it was noted that accuracy is the ratio of correctly classified instances to the total instances. Precision is the ratio of true positives to all positive instances, and recall is the ratio of true positives to all instances that are genuinely positive. All these metrics were found to exceed 0.8.

Table 2. Performance metrics of RF Classifier for flood hazard classification in Arizona.

Scenario	Performances			Hyperparameters	
	Accuracy	Precision	Recall	N° Estimators	Max Depth
Worst-case scenario	0.8	0.8	0.8	404	18
5%	0.82	0.82	0.82	201	18
10%	0.84	0.84	0.84	468	18
25%	0.88	0.88	0.88	125	18
50%	0.88	0.88	0.88	318	19
75%	0.85	0.85	0.85	271	19

Furthermore, a Confusion Matrix was provided for each threshold setting in Table 3, offering an in-depth evaluation of the model's performance. Table 4, on the other hand, displays the accuracy metrics for the A zone classification under varying threshold settings, spanning from the worst-case scenario to more forgiving criteria like the 75% threshold. The worst-case scenario yielded the peak accuracy value of 84.59%, signifying that the RF Classifier was successful in accurately categorizing a substantial number of cells into the A zone category, indicative of areas with the highest flood hazard. As the threshold setting becomes more relaxed, the accuracy diminishes, with the minimum accuracy value of 28% noted at the 75% threshold.

The Gini index was used to gauge the significance of variables across various scenarios (refer to Figure 7). The findings revealed that the Palmer Drought Severity Index consistently emerged as the most significant variable across all scenarios. Elevation, downward surface shortwave radiation, and wind speed were also identified as key variables in most scenarios. Precipitation, climate water deficit, and slope held moderate significance in certain scenarios, while variables such as soil moisture, actual evapotranspiration, and vapor pressure deficit were of low significance in most scenarios. In some scenarios, topography-related variables such as curvature, flow accumulation, and aspect held greater

significance. The snow water equivalent was consistently the least significant variable across all scenarios. Collectively, these results suggest that climate-related variables and topographical features are pivotal in predicting the target variable across different scenarios, as evidenced by their high Gini index values.

Table 3. Confusion Matrix for each threshold setting, testing sample.

Worst-Case Scenario	**D**	**X**	**AO**	**AH**	**A (A + AE)**	**5%**	**D**	**X**	**AO**	**AH**	**A (A + AE)**
D	2032	45	0	-	213	D	2464	168	0	0	58
X	217	576	0	-	251	X	234	1133	0	0	157
AO	0	0	0	-	1	AO	1	1	0	0	4
AH	-	-	-	-	-	AH	0	0	0	0	2
A (A + AE)	191	78	0	-	1477	A (A + AE)	114	183	0	0	562
10%	D	X	AO	AH	A (A + AE)	25%	D	X	AO	AH	A (A + AE)
D	2558	180	0	-	20	D	2556	207	0	0	8
X	284	1442	0	-	57	X	297	1816	0	0	7
AO	24	4	0	-	2	AO	2	5	1	0	0
AH	-	-	-	-	-	AH	0	0	0	0	1
A (A + AE)	68	202	0	-	262	A (A + AE)	30	84	0	0	67
50%	D	X	AO	AH	A (A + AE)	75%	D	X	AO	AH	A (A + AE)
D	2601	240	0	0	3	D	2667	232	0	0	1
X	285	1879	0	0	2	X	274	1865	1	0	0
AO	1	9	0	0	0	AO	3	5	0	0	0
AH	0	1	0	0	0	AH	0	1	0	0	0
A (A + AE)	9	31	0	0	20	A (A + AE)	11	12	0	0	9

Table 4. Accuracy of flood hazard classification for A zones across different thresholds.

Scenario	**Percentage Accuracy for A (A + AE)**
Worst-case scenario	85
5%	65
10%	49
25%	37
50%	33
75%	28

3.4. New Flood Hazard Maps

The calibrated RF Classifier, originally trained on the flood hazard map of Arizona, was used to generate new flood hazard maps for Utah, Colorado, and New Mexico (refer to Figure 8). The 25% scenario was chosen as the threshold setting for classification due to its consistently superior performance relative to other models. These flood hazard maps offer crucial insights to local authorities, empowering them to make well-informed decisions pertaining to flood hazard management and emergency readiness. It is noteworthy that the threshold setting employed in the creation of these maps was scenario-specific, and local authorities may opt for different configurations based on their unique requirements and priorities. By leveraging the RF Classifier and the flood hazard map of Arizona as a calibration instrument, we have showcased the potential of this methodology to be extended to other regions, offering a flexible and scalable approach for flood hazard evaluation and management.

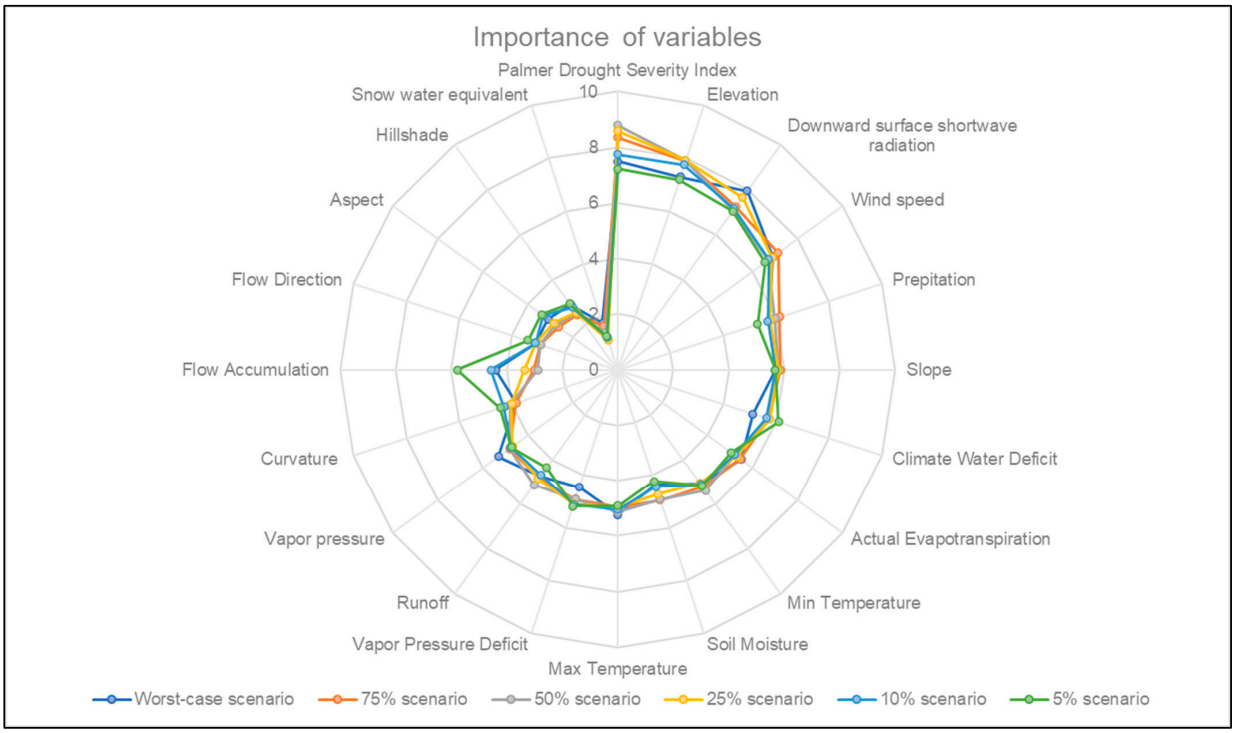

Figure 7. Variable importance based on Gini Index for different scenarios.

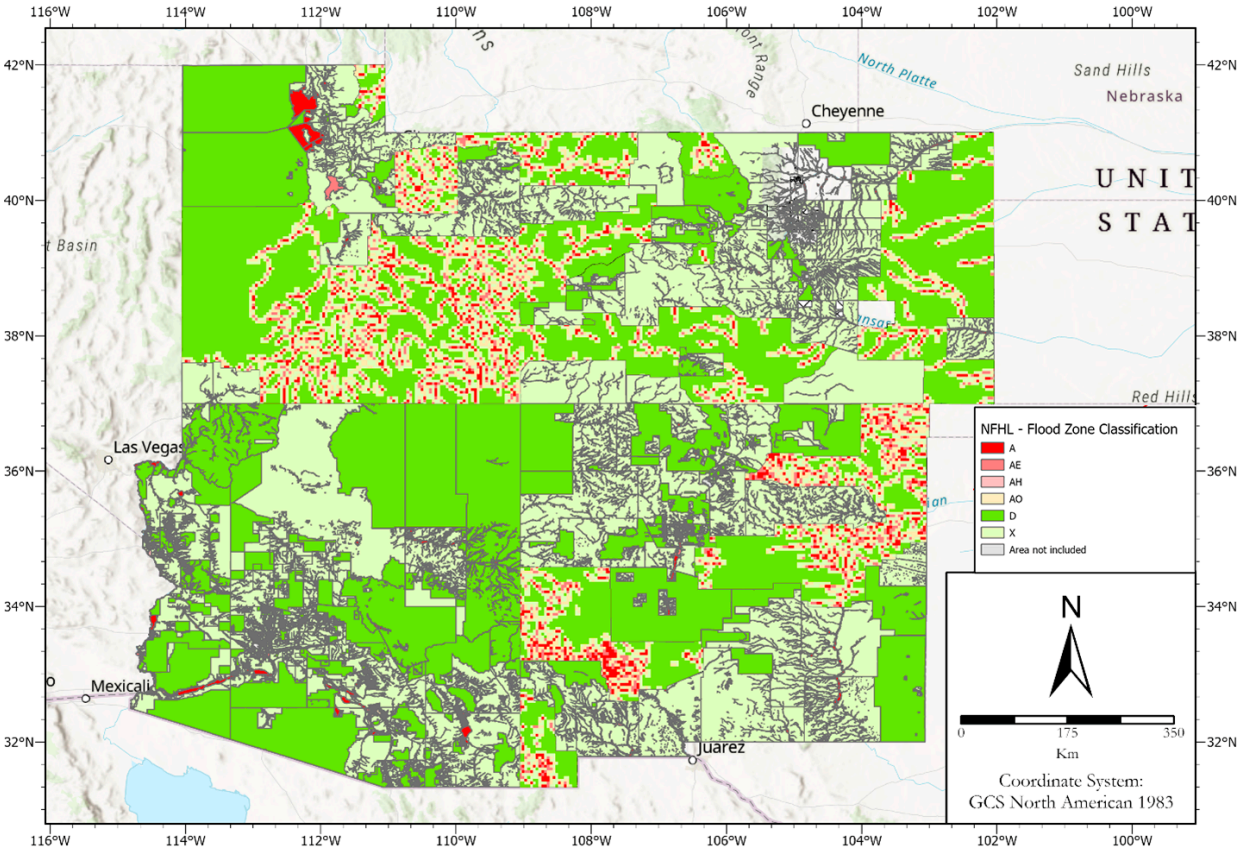

Figure 8. New flood hazard maps for Utah, Colorado, and New Mexico based on RF classification using Arizona flood hazard map calibration.

3.5. Maps Website

The results of this study, which estimated the NFHL for each cell in Arizona, New Mexico, Colorado, and Utah using a calibrated RF model with topographic and weather data are available to the public through an ArcGIS interactive map. The map allows users to easily visualize and analyze the flood hazard in their area and can be used for planning and preparedness purposes by local authorities, emergency management agencies, and residents in these regions. The map is accessible to the public at the following link: www.bit.ly/43w6PyO, accessed on 14 October 2024.

4. Discussion

While there exists a plethora of machine learning configurations for flood hazard analysis, the focus of this paper is to showcase a comprehensive approach that integrates diverse data sources and modeling techniques to provide an effective solution. The findings presented in this study offer significant insights into the application of an RF Classification methodology for flood hazard analysis, utilizing a combination of topographic and weather data. Through rigorous analysis and modelling, it has been demonstrated the potential of this approach to provide accurate flood hazard assessments, not only for Arizona but also for the neighbouring regions of New Mexico, Colorado, and Utah.

One of the key strengths of this new methodology lies in the integration of diverse data sources and the flexibility that it offers for customization based on stakeholder needs. It demonstrated one realization among many possibilities, emphasizing that stakeholders must define which machine learning approach, datasets, and tuning strategies are best suited for their specific requirements. This investigation highlights that by training machine learning models with flood hazard maps and using public remote sensing data such as the NFHL, 3DEP DEMs, and TerraClimate, flood hazard prediction can be achieved economically and efficiently. This integration allows for a comprehensive understanding of flood hazard dynamics, significantly enhancing the accuracy of our predictive models and enabling the creation of flood hazard maps on a global scale. Moreover, this methodology demonstrated scalability and flexibility by extending flood hazard analysis from Arizona to neighbouring states. This highlights the potential for our approach to be adapted and applied to diverse geographical regions, offering a versatile tool for flood hazard assessment.

The feature importance analysis conducted as part of this study revealed several key variables that significantly influenced flood hazard estimation using the RF Classification model. Among these variables, the Palmer Drought Severity Index (PDSI), elevation, downward surface shortwave radiation, wind speed, precipitation, and slope emerged as the most influential factors. The PDSI serves as a crucial indicator for flood hazard assessment by capturing long-term drought conditions, which can exacerbate flooding by drying out soil and reducing its water absorption capacity. Additionally, elevation influences flood hazard, with higher areas experiencing lower hazard as water flows away, while low-lying regions are more susceptible to inundation. Downward surface shortwave radiation affects flood hazard through its impact on evaporation rates and soil moisture levels, while wind speed intensifies precipitation patterns, particularly in coastal areas. Precipitation itself is a significant predictor of flood hazard, overwhelming drainage systems and leading to widespread flooding, especially during intense rainfall events. Lastly, slope plays a vital role by influencing surface runoff, with steeper slopes increasing erosion and flash flood hazard in mountainous terrains, while flatter areas elevate the hazard of localized flooding due to water accumulation.

However, our study also has its limitations. While our analysis benefited from multiple data sources, certain limitations exist particularly regarding the spatial resolution and coverage of available datasets. Improving the resolution and coverage of topographic and weather data could enhance the precision of flood hazard predictions. Additionally, the calibration of the RF model relied on flood hazard data from Arizona, which may not fully capture the unique characteristics of regions in New Mexico, Colorado, and Utah,

introducing biases and limitations in the accuracy of flood hazard assessments for these areas. Moreover, the classification of flood hazard cells was sensitive to threshold settings, impacting the distribution of hazard categories across different scenarios. However, to mitigate these limitations, one can integrate flood hazard maps from other states and countries and incorporate additional public remote sensing information to enhance the correlation between input and target variables, thereby improving the overall accuracy and reliability of our flood hazard assessments.

Ultimately, this new approach relies on the accuracy of the input data. While the NFHL and DEM data are highly detailed and accurate, the weather variable estimations from TerraClimate may have some errors or uncertainties. It is important to note that even though there are errors in TerraClimate, these errors are consistent across the entire world, meaning they apply uniformly in the future. The machine learning model will incorporate these constant errors, which is beneficial when estimating the Flood Risk Map. Each measurement carries some degree of error, but if these errors remain constant, they can aid in the overall estimation of flood risk. Another limitation is that this approach is based on a Random Forest (RF) model, which may not capture all the complex interactions between the input variables and flood hazard. Despite these limitations, this approach provides a valuable tool for estimating flood hazard in areas lacking NFHL classifications and can be useful for decision-makers in areas prone to flooding.

One notable advantage of this new approach lies in its applicability to regions lacking NFHL classifications. Take New Mexico, for instance, where certain counties have yet to receive NFHL designations. Through the use of DEMs and estimations of weather variables, it was possible to gauge flood hazard in these areas. Additionally, this method offers a holistic view of impacts of weather on flood hazard by aggregating the sum of various weather variables sourced from TerraClimate throughout the year. This facilitates a deeper understanding of the interplay between weather patterns and flood susceptibility in each locale. By doing so, one can reconsider the methodology for generating flood hazard maps, focusing on the most significant features identified by ML algorithms, thereby optimizing resource allocation. Ultimately, establishing a reliable model enables its deployment across diverse geographical regions worldwide.

Looking towards future research directions, several avenues can be identified. Improved data integration could involve incorporating additional data sources such as high-resolution remote sensing imagery and hydrological models, to further enhance the accuracy and granularity of flood hazard assessments. Validation and sensitivity analyses could provide insights into the robustness of predictive models and help identify sources of uncertainty. Moreover, incorporating socioeconomic factors into flood hazard models can provide a more comprehensive understanding of the potential impacts of flooding on communities, supporting more effective hazard management and adaptation strategies. Exploring advanced ML techniques such as deep learning algorithms could offer opportunities to further improve the accuracy and efficiency of flood hazard prediction models, ultimately contributing to the continued evolution of flood hazard assessment methodologies and supporting more resilient and sustainable communities in the face of increasing flood hazards.

5. Conclusions

In conclusion, this study presents an RF-based model for estimating flood hazard in Arizona, New Mexico, Colorado, and Utah using topographic and weather data. The study illustrates a step-by-step methodology, which includes obtaining the most recent version of the NFHL, creating a high-resolution flood map, and applying the RF Classification algorithm to estimate the NFHL for each cell. The study also demonstrates the advantages of this new approach including its ability to estimate flood hazard in areas lacking NFHL classifications, providing a comprehensive picture of the overall impact of weather on flood hazard in each area. However, the study acknowledges some limitations including the

accuracy of the input data and the potential inability of the RF model to capture all the complex interactions between the input variables and flood hazard.

This research has important implications for decision-makers in areas prone to flooding, as it provides a valuable tool for estimating flood hazard and can aid in planning and preparedness efforts. The availability of the results through an ArcGIS interactive map makes the data accessible to the public and can facilitate local authorities, emergency management agencies, and residents in these regions to make informed decisions about flood hazard. Further research can be conducted to refine and improve the accuracy and robustness of this new approach, and to explore other ML algorithms that may provide even better results. Also, the methodology presented in this study provides a useful framework for assessing flood hazard in other regions and could be extended to areas outside of Arizona, New Mexico, Colorado, and Utah. The study highlights the potential for integrating different types of data such as topographic and weather data to provide a comprehensive picture of flood hazard and could pave the way for future research in this area.

Machine learning is a powerful tool that can greatly enhance the stakeholder's process for flood hazard management. By leveraging ML algorithms, one can estimate flood hazard in areas lacking accurate data, while providing decision-makers with a comprehensive picture of the overall impact of weather on flood hazard in each region. This can help local authorities, emergency management agencies, and residents in flood-prone regions to plan and prepare for future flood events. Moreover, ML-based flood hazard estimation can be made available to the public through interactive maps, which can be accessed for free by anyone. As ML algorithms continue to evolve, one can expect to see further improvements in the accuracy and robustness of flood hazard estimation models. The availability of high-quality data and the continued development of machine learning techniques will allow users to refine models and improve their understanding of the complex interactions between topography, weather patterns, and flood hazard. As the technology continues to advance and data becomes more readily available, one can expect to see significant advancements in this field. By making these tools accessible to the public and continually refining obtained models, we can work together to better understand and prepare for future flood events.

Author Contributions: Conceptualization, H.L.V.-Q.; Methodology, H.L.V.-Q.; Investigation, H.L.V.-Q.; Writing—original draft, H.L.V.-Q., P.G.-C., R.V.-P. and T.P.A.F.; Writing—review & editing, J.E.M. and L.B.; Visualization, P.G.-C.; Supervision, P.G.-C., R.V.-P., T.P.A.F., H.G., D.G., J.B.V., J.E.M. and L.B. All authors have read and agreed to the published version of the manuscript.

Funding: This research received no external funding.

Data Availability Statement: Data is contained within the article.

Conflicts of Interest: The authors declare no conflict of interest.

References

1. Tellman, B.; Sullivan, J.A.; Kuhn, C.; Kettner, A.J.; Doyle, C.S.; Brakenridge, G.R.; Erickson, T.A.; Slayback, D.A. Satellite imaging reveals increased proportion of population exposed to floods. *Nature* **2021**, *596*, 80–86. [CrossRef] [PubMed]
2. Li, J.; Bortolot, Z.J. Quantifying the impacts of land cover change on catchment-scale urban flooding by classifying aerial images. *J. Clean. Prod.* **2022**, *344*, 130992. [CrossRef]
3. Prettenthaler, F.; Kortschak, D.; Albrecher, H.; Köberl, J.; Stangl, M.; Swierczynski, T. Can 7000 Years of flood history inform actual flood risk management? A case study on Lake Mondsee, Austria. *Int. J. Disaster Risk Reduct.* **2022**, *81*, 103227. [CrossRef]
4. Khosravi, K.; Rezaie, F.; Cooper, J.R.; Kalantari, Z.; Abolfathi, S.; Hatamiafkoueieh, J. Soil water erosion susceptibility assessment using deep learning algorithms. *J. Hydrol.* **2023**, *618*, 129229. [CrossRef]
5. Jongman, B. Effective adaptation to rising flood risk. *Nat. Commun.* **2018**, *9*, 1986. [CrossRef] [PubMed]
6. Dottori, F.; Szewczyk, W.; Ciscar, J.-C.; Zhao, F.; Alfieri, L.; Hirabayashi, Y.; Bianchi, A.; Mongelli, I.; Frieler, K.; Betts, R.A.; et al. Increased human and economic losses from river flooding with anthropogenic warming. *Nat. Clim. Chang.* **2018**, *8*, 781–786. [CrossRef]

7. Davenport, F.V.; Burke, M.; Diffenbaugh, N.S. Contribution of historical precipitation change to US flood damages. *Proc. Natl. Acad. Sci. USA* **2021**, *118*, e2017524118. [CrossRef]
8. Powell, T.; Hanfling, D.; Gostin, L.O. Emergency preparedness and public health: The lessons of Hurricane Sandy. *Jama* **2012**, *308*, 2569–2570. [CrossRef]
9. Seligman, J.; Felder, S.S.; Robinson, M.E. Substance Abuse and Mental Health Services Administration (SAMHSA) Behavioral Health Disaster Response App. *Disaster Med. Public Health Prep.* **2015**, *9*, 516–518. [CrossRef]
10. Chen, Y. Flood hazard zone mapping incorporating geographic information system (GIS) and multi-criteria analysis (MCA) techniques. *J. Hydrol.* **2022**, *612*, 128268. [CrossRef]
11. Mudashiru, R.B.; Sabtu, N.; Abustan, I.; Balogun, W. Flood hazard mapping methods: A review. *J. Hydrol.* **2021**, *603*, 126846. [CrossRef]
12. Tyler, J.; Sadiq, A.-A.; Noonan, D.S.; Entress, R.M. Decision Making for Managing Community Flood Risks: Perspectives of United States Floodplain Managers. *Int. J. Disaster Risk Sci.* **2021**, *12*, 649–660. [CrossRef]
13. Kam, P.M.; Aznar-Siguan, G.; Schewe, J.; Milano, L.; Ginnetti, J.; Willner, S.; McCaughey, J.W.; Bresch, D.N. Global warming and population change both heighten future risk of human displacement due to river floods. *Environ. Res. Lett.* **2021**, *16*, 044026. [CrossRef]
14. Chaminé, H.I.; Pereira, A.J.S.C.; Teodoro, A.C.; Teixeira, J. Remote sensing and GIS applications in earth and environmental systems sciences. *SN Appl. Sci.* **2021**, *3*, 870. [CrossRef]
15. Xian, S.; Lin, N.; Hatzikyriakou, A. Storm surge damage to residential areas: A quantitative analysis for Hurricane Sandy in comparison with FEMA flood map. *Nat. Hazards* **2015**, *79*, 1867–1888. [CrossRef]
16. National Research Council; Board on Earth Sciences and Resources; Mapping Science Committee; Water Science and Technology Board; Committee on FEMA Flood Maps. *Mapping the Zone: Improving Flood Map Accuracy*; National Academies Press: Washington, DC, USA, 2009.
17. Woznicki, S.A.; Baynes, J.; Panlasigui, S.; Mehaffey, M.; Neale, A. Development of a spatially complete floodplain map of the conterminous United States using random forest. *Sci. Total Environ.* **2019**, *647*, 942–953. [CrossRef]
18. Sun, Q.; Miao, C.; Duan, Q.; Ashouri, H.; Sorooshian, S.; Hsu, K.-L. A Review of Global Precipitation Data Sets: Data Sources, Estimation, and Intercomparisons. *Rev. Geophys.* **2018**, *56*, 79–107. [CrossRef]
19. Zheng, F.; Tao, R.; Maier, H.R.; See, L.; Savic, D.; Zhang, T.; Chen, Q.; Assumpção, T.H.; Yang, P.; Heidari, B.; et al. Crowdsourcing Methods for Data Collection in Geophysics: State of the Art, Issues, and Future Directions. *Rev. Geophys.* **2018**, *56*, 698–740. [CrossRef]
20. Association of State Floodplain Managers. *Flood Mapping for the Nation: A Cost Analysis for Completing and Maintaining the Nation's NFIP Flood Map Inventory*; Association of State Floodplain Managers: Madison, WI, USA, 2020.
21. Penning-Rowsell, E.; Becker, M. *Flood Risk Management: Case Studies of Governance, Policy and Communities*; Routledge: New York, NY, USA, 2019.
22. Antzoulatos, G.; Kouloglou, I.-O.; Bakratsas, M.; Moumtzidou, A.; Gialampoukidis, I.; Karakostas, A.; Lombardo, F.; Fiorin, R.; Norbiato, D.; Ferri, M.; et al. Flood Hazard and Risk Mapping by Applying an Explainable Machine Learning Framework Using Satellite Imagery and GIS Data. *Sustainability* **2022**, *14*, 3251. [CrossRef]
23. Kavakiotis, I.; Tsave, O.; Salifoglou, A.; Maglaveras, N.; Vlahavas, I.; Chouvarda, I. Machine Learning and Data Mining Methods in Diabetes Research. *Comput. Struct. Biotechnol. J.* **2017**, *15*, 104–116. [CrossRef]
24. Karim, F.; Armin, M.A.; Ahmedt-Aristizabal, D.; Tychsen-Smith, L.; Petersson, L. A Review of Hydrodynamic and Machine Learning Approaches for Flood Inundation Modeling. *Water* **2023**, *15*, 566. [CrossRef]
25. Nevo, S.; Morin, E.; Gerzi Rosenthal, A.; Metzger, A.; Barshai, C.; Weitzner, D.; Voloshin, D.; Kratzert, F.; Elidan, G.; Dror, G. Flood forecasting with machine learning models in an operational framework. *Hydrol. Earth Syst. Sci.* **2022**, *26*, 4013–4032. [CrossRef]
26. Shrivastava, D.; Sanyal, S.; Maji, A.K.; Kandar, D. Chapter 17—Bone cancer detection using machine learning techniques. In *Smart Healthcare for Disease Diagnosis and Prevention*; Paul, S., Bhatia, D., Eds.; Academic Press: Cambridge, MA, USA, 2020; pp. 175–183. [CrossRef]
27. Gigović, L.; Pourghasemi, H.R.; Drobnjak, S.; Bai, S. Testing a new ensemble model based on SVM and random forest in forest fire susceptibility assessment and its mapping in Serbia's Tara National Park. *Forests* **2019**, *10*, 408. [CrossRef]
28. Zhou, L.; Dang, X.; Sun, Q.; Wang, S. Multi-scenario simulation of urban land change in Shanghai by random forest and CA-Markov model. *Sustain. Cities Soc.* **2020**, *55*, 102045. [CrossRef]
29. Ayala-Izurieta, J.E.; Márquez, C.O.; García, V.J.; Recalde-Moreno, C.G.; Rodríguez-Llerena, M.V.; Damián-Carrión, D.A. Land cover classification in an ecuadorian mountain geosystem using a random forest classifier, spectral vegetation indices, and ancillary geographic data. *Geosciences* **2017**, *7*, 34. [CrossRef]
30. Kim, J.-C.; Lee, S.; Jung, H.-S.; Lee, S. Landslide susceptibility mapping using random forest and boosted tree models in Pyeong-Chang, Korea. *Geocarto Int.* **2018**, *33*, 1000–1015. [CrossRef]
31. Schoppa, L.; Disse, M.; Bachmair, S. Evaluating the performance of random forest for large-scale flood discharge simulation. *J. Hydrol.* **2020**, *590*, 125531. [CrossRef]

32. Abedi, R.; Costache, R.; Shafizadeh-Moghadam, H.; Pham, Q.B. Flash-flood susceptibility mapping based on XGBoost, random forest and boosted regression trees. *Geocarto Int.* **2022**, *37*, 5479–5496. [CrossRef]
33. Collins, E.L.; Sanchez, G.M.; Terando, A.; Stillwell, C.C.; Mitasova, H.; Sebastian, A.; Meentemeyer, R.K. Predicting flood damage probability across the conterminous United States. *Environ. Res. Lett.* **2022**, *17*, 034006. [CrossRef]